Large Amplitude Solitary Waves in and near the Earth's Magnetosphere, Magnetopause and Bow Shock: Polar and Cluster Observations

C. Cattel1, C. Neiman, J. Dombeck, J. Crumley, J. Wygant
School of Physics and Astronomy, University of Minnesota, Minneapolis, MN 55455 USA

C. A. Kletzing
Dept. of Physics and Astronomy, University of Iowa, Iowa City, IA 52242 USA

W. K. Peterson
Lockheed Martin Space Sciences Laboratory, Palo Alto, CA 94304 USA

F.S. Mozer
Space Sciences Laboratory, University of California, Berkeley, CA 94720 USA

Mats André
Swedish Institute for Space Physics, Uppsala, Sweden

The paper is for a special issue associated with the Tromso Nonlinear Waves and Chaos Workshop.

Proofs and offprint requests should be sent to:
Prof. C. Cattell, School of Physics and Astronomy, 116 Church St. SE, University of Minnesota, Minneapolis, MN 55455 USA (cattell@belka.space.umn.edu)

Abstract. Solitary waves with large electric fields (up to 100's of mV/m) have been observed throughout the magnetosphere and in the bow shock. We discuss observations by Polar at high altitudes (~ 4-8 R_E), during crossings of the plasma sheet boundary and cusp, and new measurements by Polar at the equatorial magnetopause and by Cluster near the bow shock, in the cusp and at the plasma sheet boundary. We describe results of a statistical study of electron solitary waves observed by Polar at high altitudes. The waves have velocities from ~1000km/s to >2500 km/s. Observed scale sizes are on the order of 1-10λ_D with $e\phi/kT_e$ from ~0.01 to O(1). The average speed of solitary waves at the plasma sheet boundary is faster than those observed in the cusp and at cusp injections. The amplitude increases with both velocity and scale size. These observations are all consistent with the identification of the solitary waves as electron hole modes. We also report the discovery of solitary waves at the magnetopause, observed in Polar data obtained at the subsolar equatorial magnetopause. Both positive and negative potential structures have been observed with amplitudes up to ~25 mV/m. The velocities range from 150 km/s to >2500 km/s, with scale sizes the order of a kilometer (comparable to the Debye length). Initial observations of solitary waves by the four Cluster satellites are utilized to discuss the scale sizes and time variability of the regions where the solitary waves occur.

1. Introduction

Solitary waves have been identified throughout the Earth's magnetosphere at narrow boundaries, such as the plasma sheet boundary (Matsumoto et al., 1994; Franz et al., 1998; Cattell et al., 1999) and the bow shock (Bale et al., 1998; Mangeney et al., 1999), and in strong currents, such as those associated with auroral acceleration region (Temerin et al., 1982; Bostrom et al., 1988; Mozer et al., 1997; Ergun et al., 1998). They have also been seen at the high altitude polar cap boundary (Tsurutani et al., 1998), at high altitude cusp injections (Cattell et al., 2001b), and within the solar wind (Magnenay et al., 1999). Recently (Cattell et al, 2001c), been reported the first observations ofo solitary waves at the magnetopause. Almost all of these observations have been of electron solitary waves, which are seen both at high and low altitudes and are observed for wide range of f_{ce}/f_{pe}. In contrast, to date, ion solitary waves have only been observed in the auroral zone at low altitudes in the region where $f_{ce}/f_{pe}>>1$. Recent studies of ion solitary waves in the auroral zone have been presented by Bounds et al. (1999), Crumley et al.(2001) and Dombeck et al. (2001).

In this paper, we describe results of a statistical study of large amplitude electron solitary waves observed at plasma sheet boundary, and at the high altitude cusp and cusp injections using the Polar EFI instrument. We also present examples of solitary waves at the magnetopause obtained as the Polar orbit precessed into the subsolar magnetopause. In addition, we show initial examples of solitary waves from the four Cluster satellites in several different regions of the magnetosphere.

The electric field and spacecraft potential measurements utilized herein for the Polar studies were made by the double probe electric field instrument (Harvey et al., 1995). This instrument, which saturates at ~1 V/m, obtains 3d measurements of the electric field in bursts (waveform capture) of high time resolution data. In addition to the

electric field (potential difference between opposing probes), the spacecraft potential was utilized to indicate changes in density (Pederson, 1995). The delay times between signals at opposing probes were examined using a cross-correlation analysis to estimate the propagation speed of electric field structures, utilizing an automatic program that examined the parallel component of the electric field data in magnetic field-aligned coordinate system. The largest velocities which can be measured (~2500 km/s) correspond to the resolution of the time delay and depend on the boom orientation. Events where no time delay could be measured are included in statistics as 'infinite velocity.' The automatic program used to calculate velocity also determines the structure width and solitary wave amplitude. Note that the method yields scale sizes which are approximately a factor of 4 larger than those obtained when the potential is fit to a Gaussian because the duration of the solitary wave is based on the gradient in the parallel electric field changing sign rather than on the Gaussian half-width. Details of this procedure and sample cross-correlation analysis are described elsewhere (Dombeck et al., 2001). The AC magnetic field from the search coils (Gurnett et al., 1995) were sampled in the burst memory at the same rate as the electric field. DC magnetic field data, obtained from the fluxgate magnetometers (Russell et al., 1995), were utilized to determine location of boundaries. In addition, ion composition measurements, made by the TIMAS instrument (Shelley et al., 1995), were examined to determine the probable source region and plasma characteristics. Hydra (Scudder et al., 1995) provided additional information on the particle distributions and moments in these regions.

The data for the Cluster study were obtained as the Cluster satellites traversed the bow shock, magnetopause, cusp and the plasma sheet boundary. The electric field and spacecraft potential measurements were made by the double probe electric field instruments (Gustaffson et al., 1988), which were designed to obtain bursts of high time resolution data in many different modes. Electric field data at frequencies from dc to Nyquist frequency of 9 kHz were obtained in the waveform captures described herein. Single probe measurements were not transmitted for the events described herein, so solitary wave velocities could not be measured. The spacecraft potential was used to provide preliminary identification of the various boundaries and for determining boundary orientation and velocity. Note that the Cluster instruments only measure the electric field in the spin plane (approximately the ecliptic plane).

2. Polar discovery of solitary waves at the magnetopause

The precession of the Polar orbit so that apogee is in the equatorial plane has enabled a study of the subsolar, low latitude magnetopause with a modern suite of instruments. During March and April, 2001, Polar repeatedly encountered the magnetopause. Cattell et al (2001c) reported the discovery of solitary waves in waveform capture data obtained at these magnetopause crossings. The three -dimensional nature of the Polar electric field instrument was critical for this discovery because the dominant component of the geomagnetic field is in the Z direction (out of the ecliptic plane). Two-dimensional instruments, which measure the component of the electric field in the x-y (ecliptic) plane, would not usually be able to observe solitary waves.

An example of an equatorial magnetopause crossing on 4/2/2001 at 9.4 Re and 11.6 MLT when the interplanetary magnetic field (IMF) was southward is presented in Figure 1. The transition from the magnetosphere (low density) to the magnetosheath (high density) can be clearly seen in the negative of the spacecraft potential (fifth panel) which is proportional to density. The transition is also clear in the magnetic field in geocentric solar magnetospheric (GSM) coordinates (panels 6-9). The electric field waveform capture was obtained throughout the magnetopause current layer, and part of the ~34s burst extended into the magnetosheath. The two perpendicular components in magnetic field-aligned coordinates (shown in panels 3 and 4) have very large amplitude waves (up to ~200 mV/m peak-to-peak). In order to see the solitary wave signatures, it is necessary to look at the parallel component for shorter intervals, as shown in the top two panels, which plot 0.09s intervals from the burst. The bipolar signature, which is typical of solitary waves, can be clearly seen. In the top panel, in addition to a train of spikes, several isolated solitary waves with amplitudes up to 10 mV/m can be seen. The second panel shows an isolated solitary wave with an amplitude of ~25 mV/m. The solitary wave speeds were too high for a time delay to be observable in this low data rate (1600 samples/s) burst.

Figure 2 displays the x and z components of the electric field and the x component of the search coil magnetic field data in field-aligned coordinates and their Fourier transforms. Most of the power in the perpendicular electric field is at frequencies of <50 Hz, consistent with lower hybrid waves as has been previously observed (Treumann et al., 1995; Cattell et al., 1995). The ac magnetic field has bursts of waves near the electron cyclotron frequency in the magnetic field minima. These waves can also be seen in the electric field when the larger amplitude low frequency electrostatic waves and the broadband signature due to the solitary waves don't mask them.

Waveform captures were obtained near two magnetopause crossings on 3/23/2001 at ~9Re and 12 MLT. The first wave form capture (from ~01:36:14-01:36:19UT) occurred during a partial crossing of the magnetopause, just a few minutes prior to a complete outbound magnetopause crossing (at ~01:39:10UT) during southward IMF. Figure 3 shows the data from this event. The parallel electric field component for an interval of 0.4s is plotted in the top panel, and the negative of the spacecraft potential and the magnetic field in the bottom five panels. At the time of the waveform capture, the density was increasing (as indicated by the spacecraft potential), and the y and z components and the magnitude of the magnetic field were decreasing, as expected if the satellite is moving from the magnetosphere towards the magnetosheath. The signatures of solitary waves with amplitudes of ~1 mV/m to ~8 mV/m can be seen in the top panel. The solitary waves had speeds of ~800->2000km/s. The second crossing from the magnetosheath into the magnetosphere at 03:32UT is shown in Figure 4 (same format as Fig. 3). Solitary waves can be seen in the top panel which shows a short interval during the waveform capture which was taken from 03:32:19-03:32:51, on the magnetospheric side of the magnetopause current layer. Note that one of the solitary waves is a tripolar rather than bipolar structure. Tripolar solitary waves were observed in other events, as well as in the Cluster data described below.

Additional examples are presented by Cattell et al. (2001c) who also discussed results of a study of all ten high time resolution bursts obtained at and near the subsolar magnetopause. Solitary waves were observed in all except one. Solitary waves velocities

from ~150 km/s to >2000 km/s and amplitudes of up to 25 mV/m were observed. The scale sizes are the order of a kilometer, comparable to the Debye length for the usual range of plasma conditions at the magnetopause. Although most solitary waves were positive potential structures (consistent with the electron hole interpretation), there were also some negative potential structures. The fact that very low velocities and negative potential structures were sometimes observed suggests that there may be other types of solitary waves at the magnetopause. The wide range of velocities, however, is also consistent with the fact that mixtures of ionospheric, magnetosheath and magnetospheric particles occur in the magnetopause current layer.

3. Polar statistical studies of electron solitary waves

Observations of large amplitude solitary waves for a number of Polar crossings of the plasma sheet boundary, cusp and cusp particle injections at radial distances of ~4-9 R_e have been presented by Cattell et al. (1999; 2001a; 2001b). These studies showed that the high altitude electron solitary waves have velocities from ~1000km/s to >2500 km/s and amplitudes up to 200 mV/m. More detailed discussion of the relationship of the velocity to the particle characteristics can be found in these references. For the small set of events studied, the amplitude increased with both the velocity and the scale size, consistent with electron hole modes. The solitary waves were stable based on the criterion developed by Muschietti et al.(1999). Herein we discuss the results of a new statistical study of high altitude solitary waves observed by the Polar EFI.

All the high time resolution (8000 samples/s) waveform capture intervals which were obtained at high altitudes during 1997 have been examined for solitary waves utilizing the method of Dombeck et al. (2001). The ion composition data from TIMAS and the plasma data from Hydra were examined to classify each interval as a plasma sheet boundary, cusp injection, cusp, or other region. A cusp injection event was defined as a case where the waveform capture was obtained at the leading edge of a velocity-dispersed cusp ion injection. This study was designed to provide statistical information on the characteristics of high altitude solitary waves and to determine whether these characteristics varied depending on the magnetospheric region.

Figure 5 presents a histogram of the solitary wave speed for the three spatial regions. Note that ‘Inf’ refers to cases which were moving so rapidly (usually >2500 km/s) that no time delay could be measured. These cases are not included in the average. The average speed of solitary waves in the plasma sheet boundary was ~1900 km/s, significantly larger than the average speed of solitary waves in the cusp and at cusp injections (~1400 km/s). That solitary waves in the plasma sheet boundary propagate faster is even clearer when one examines the percentage of the solitary waves for which no time delay could be measured. Almost half were in the ‘Inf’ category, whereas, in the cusp injection and cusp event sets, <~20% were moving too fast to be timed. This is consistent with the interpretation that the structures are electron holes and the fact that the electron temperature (and velocity) is lower in the cusp than in the plasma sheet boundary.

The scale size normalized to the Debye length determined using the Hydra key parameter electron density and temperature were also examined for each region. The average width in the plasma sheet boundary is ~1-2 λ_D; and, in the cusp (cusp injection), it is ~5(8) λ_D. This difference may not be significant because so many plasma sheet

events had 'infinite velocity'; therefore, only a minimum scale size could be computed. These widths are consistent with Goldman et al. (1999) who predicted scale sizes of 6-8λ_D. Note, however, that their simulations were for the strongly magnetized case, whereas the high altitude events are weakly magnetized.

A histogram of the amplitude of the solitary waves for all the high altitude events is shown in Figure 6. Although most of the observed solitary waves have potentials of <5V, there is a long tail with events out to amplitudes of 100 V (not shown). The average normalized amplitudes, $e\phi/kT_e$, are the order of 0.01, with some events having amplitudes on the order of 1. The average amplitude was larger for the plasma sheet boundary events than for the cusp events and very large amplitude waves were more common there. The relationship between potential amplitude and width is shown in Figure 8. The amplitudes and scale sizes for the events with 'Inf' velocity, plotted as asterisks, are lower bounds. There is a clear tendency for amplitude to increase with width, which is in agreement with the prediction for a 1d BGK electron hole, but is opposite to the dependence predicted for a 1d, small amplitude acoustic soliton.

4. Cluster observations of solitary waves

Preliminary studies of the Cluster waveform capture data have provided many examples of solitary waves and other nonlinear waveforms, at and near the bow shock, at the plasma sheet boundary, in the cusp and during high altitude auroral zone crossings. The Cluster data provide the opportunity to determine where, within a boundary or current sheet, solitary waves occur, the time and spatial variability of the occurrence and properties of solitary waves, and their relationship to other type of waves and wave packets. Examples taken on three days at different locations are presented below.

On March 7, 2001, three of the Cluster satellites collected waveform captures at ~8.2 R_e and ~9 MLT at the outer edge of the cusp. An overview of the complete waveform capture for 1 component of the electric field and its Fourier transform from SC2, SC3, and SC4 is shown in Figure 8a. It is clear that the character of the waves is quite different on the 3 satellites. The waves observed on SC3 had the largest amplitude (up to 40 mV/m) and were the most spiky, including numerous solitary waves. Although all three satellites observed waves at 2kHz, close to the electron cyclotron frequency, and harmonics, these waves were strongest on SC4. Of the three satellites with waveform captures at this time, SC3 was closest to the equatorial plane and SC4 farthest from the equatorial plane. Several snapshots during the interval (Figure 8b-8d) show the highly variable character of the waves. The ~0.1s interval in 8b was taken when the waves on SC2 were very small amplitude (<1mV/m) and solitary waves were observed by both SC3 (up to ~10mV/m) and SC4 (up to ~4mV/m). In addition, SC4 observed quasi-monochromatic waves at ~2kHz (f_{ce} was ~2.8kHz). The ~0.05s interval in Figure 8c, which occurred at the end of the waveform capture interval when data from SC4 were no longer available, has examples of solitary waves from both SC2 and SC3. Note that the solitary wave on SC2 was much lower amplitude consistent with the fact that the electric field perturbations on SC2 were small compared to the other satellites throughout the waveform capture. Figure 8d shows a period where the waves on both SC2 and SC4 were small amplitude and solitary waves with amplitudes up to ~25 mV/m were seen on SC3.

On March 3, 2001, the Cluster satellites were at ~15R_e near noon, close to the bow shock, and all four obtained waveform captures. Figure 9a shows an overview of the observations with one component of the electric field and its Fourier transform from each satellite. All four spacecraft see intense, bursty wave packets with amplitudes up to ~200 mV/m. SC 1, which is farthest from the equatorial plane, sees more continuous wave packets than the other spacecraft. Wave power maximizes between ~2 and 4 kHz throughout much of this interval. Figure 9b shows data from an ~0.6s period. The highly variable modulation of the waves suggests complex nonlinear interactions which vary over the ~400 – 900 km separations of the satellites. In an ~0.02s interval shown in Figure 9c, all 4 satellites observe wave packets with comparable amplitudes and frequencies. SC3 observes a solitary structure at ~07:17:05.885. There were also large-scale structures in the spacecraft potential in the interval around the time of the waveform captures. Timing of several discontinuities seen in the spacecraft potential indicated that these large-scale structures were moving at speeds of ~300 km/s, primarily anti-sunward, with a small duskward component. The structures were observed first by SC2 and SC3, then SC4, and finally SC1.

Cluster encountered the high altitude auroral zone (plasma sheet) at a radial distance of ~4.2R_e at 21:30 MLT and ~62°ILAT (south) on March 31, 2001 at ~6:44 UT. The magnetosphere was highly compressed at this time, and the RAPID instrument observed an intense injection of electrons approximately 14 minutes earlier (Baker et al., 2001). Figure 10 shows one component of the waveform capture electric field data from the four satellites indicating that all observed large-amplitude waves and that the types of waves are quite variable. Figure 11 plots an approximately 0.03 second interval from each satellite to illustrate that solitary waves were detected at all four locations, with amplitudes often reaching 500-750 mV/m. These are much larger than the previously reported largest solitary waves at high altitudes (Cattell et al., 2001a) which were 200 mV/m and observed by Polar at ~5Re. Although the solitary waves are usually distinct individual pulses, they sometimes occur in wave trains (as near 06:44:01.5 on SC3). As discussed in relationship to previous examples on both Polar and Cluster, although symmetric bipolar pulses are the predominant signature, asymmetric solitary waves, and tri-polar and more complex shapes are also seen.

An example of waveform capture data obtained in the plasma sheet at ~19R_e and 1.8MLT is displayed in Figure 12 (same format as Figure 8a). A narrow band emission at ~1.7kHz occurred at all locations. The waves at all four locations have amplitudes from ~20-40mV/m with peak power at the lowest frequency. The smallest amplitudes were observed by SC4 which is the most dawnward and the largest, at the end of the interval, by SC1which was most earthward.

5. Discussion and Conclusions

We have described three studies of solitary waves which are most commonly observed as bipolar pulses in the electric field parallel to the background magnetic field and which are ubiquitous in boundaries and other regions with strong currents and/or electron beams. The Polar observations at the subsolar, equatorial magnetopause have provided the first evidence for the occurrence of solitary waves in and near the magnetopause current layer. Solitary waves at the magnetopause are occur both as individual spikes and in trains of spikes with amplitudes up to ~25 mV/m, scale sizes the

order of a kilometer (comparable to the Debye length) and velocities from ~150 km/s to >2000 km/s. They are often associated with very large amplitude waves in either or both the electric and magnetic fields. Although most of the observed signatures are consistent with an electron hole mode, the events with very low velocities and the few negative potential structures may be indicative of a second type of solitary wave in the magnetopause current layer. Simulations have shown that electron holes interact strongly with electrons (Omura et al., 1996; Goldman et al., 1999; and references therein); therefore, the solitary waves may be an important source of dissipation and diffusion at the magnetopause.

The statistical study described herein of high altitude solitary waves observed by the Polar EFI provided information on the differences between of properties of solitary waves at the plasma sheet boundary, cusp injections and the cusp. No significant differences were observed between the properties within the cusp and at cusp injections. The average speed for the plasma sheet boundary events was significantly faster the average speed in the cusp events. The statistical results on the scale sizes and potentials were limited by the fact that, for events with zero time delay, only a lower limit on the potential and scale size could be obtained. Given this limitation, the observations are consistent with the conjecture that the scale sizes of the solitary waves are the order of 1-10 Debye lengths in all regions, and that the potentials were larger in the plasma sheet boundary. We did not address the shape of the solitary waves. Franz et al. (2000) described results of a statistical study of solitary waves observed at high altitude on Polar by the PWI instrument. They concluded that the ratio of parallel to perpendicular scale size depended on (f_{ce}/f_{pe}), and with the perpendicular scale size increasing with respect to the parallel scale size as (f_{ce}/f_{pe}) became less than one.

Because all previous solitary wave observations have been made by single spacecraft, it has not been possible to determine the spatial and temporal relationship between regions within the boundaries and the occurrence of solitary waves. Preliminary results from the four Cluster satellites have given a glimpse of the spatial and temporal variability of the occurrence of solitary waves and their association with other wave modes. In all the events studied, significant differences were observed in the waveforms observed simultaneously at the four locations separated by ~1000km. Cluster has observed the largest amplitude solitary waves (750 mV/m) in the outer magnetosphere in association with a highly compressed magnetosphere.

ACKNOWLEDGEMENTS. Analysis of Polar electric and magnetic field data was supported by the NASA under grants NAG 5-3182, NAG5-3217, and NAG5-7885. J. Dombeck was supported by NASA GSRP NGT5-50251 and J. Crumley by NGT5-50293. Analysis of the Cluster electric field data was supported by NAG5-9985. Analysis of HYDRA data at . University of Iowa was performed under NASA grant number NAG5-2231 and DARA grant 50 OC 8911 0. We would also like to thank C. T. Russell for use of the fluxgate magnetometer data and J. Vernetti for work on the Cluster burst-mode software. C. Cattell is a Cotrell Scholar. Her participation in this workshop was supported by Research Corporation.

REFERENCES

Bale, S. et al., Bipolar electrostatic structures in the shock transition region: Evidence of electron phase space holes, *Geophys. Res. Lett*., **25**, 2929, 1998.

Bostrom, R. et al., Characteristics of solitary waves and double layers in the magnetospheric plasma, *Phys. Rev. Lett***., 61**, 82, 1988.

Bounds, S. et al., Solitary potential structures associated with ion and electron beams near 1 R_e, *J. Geophys. Res*., **104**, 28709, 1999.

C. Cattell, J. Wygant, F. Mozer, T. Okada, S. Kokubun and T. Yamamoto, ISEE-1 and Geotail observations of low frequency waves at the magnetopause, *J. Geophys. Res.* **100**, 11823, 1995.

Cattell, C. et al., Observations of large amplitude parallel electric field wave packets at the plasma sheet boundary, *Geophys. Res. Lett***., 25**, 857-900, 1998.

Cattell, C. et al., Comparisons of Polar satellite observations of solitary wave velocities in the plasma sheet boundary and the high altitude cusp to those in the auroral zone, *Geophys. Res. Lett*., **26**, 425-428, 1999.

Cattell, C. et al., Comparison of solitary waves and wave packets observed at plasma sheet boundary to results from the auroral zone, *Phys. And Chem. of the Earth*, **26**,97, 2001a.

Cattell, C., J. Crumley, J. Dombeck, R. Lysak, C. Kletzing , W.K.Peterson, and H. Collin, Polar Observations Of Solitary Waves At High And Low Altitudes And Comparison To Theory, *Advances in Space Research*, in press, 2001b.

Cattell, C., J. Crumley, J. Dombeck, J. Wygant and F. S. Mozer, Polar observations of solitary waves at the Earth's magnetopause, submitted to *Geophys. Res. Lett***.,** 2001c.

Crumley, J., C. Cattell and R. Lysak, and J. Dombeck, Studies of ion solitary waves using simulations including hydrogen and oxygen beams, *J. Geophys. Res*., **106**, 6007, 2001.

Dombeck, J., C. Cattell, J. Crumley, W. Peterson, H. Collin, and C. Kletzing, Observed trends in auroral zone ion solitary wave structure characteristics using data from Polar, *J. Geophys. Res*., **106** , 19,013, 2001.

Ergun, R. et al., FAST satellite observations of large-amplitude solitary wave structures, *Geophys. Res. Lett*., **25**, 2041-2044, 1998.

Franz, J., P. Kintner, and J. Pickett, Polar observations of coherent electric field structures, *Geophys. Res. Lett*., **25**, 1277-1280, 1998.

Franz, J., P. Kintner, and J. Pickett, On the perpendicular scale size of electron phase space holes, *Geophys. Res. Lett*., **27**, 169-172, 2000.

Harvey, P. et al., The Electric Field Instrument on the Polar Satellite, in *The Global Geospace Mission*, C.T. Russell, ed., p. 583, 1995.

Goldman, M., M. Oppenheim, and D. Newman, Nonlinear two-stream instabilities as an explanation for auroral biploar wave structures, *Geophys. Res. Lett*., **26**, 1821-1824, 1999.

G. Gustafsson, et al., The spherical probe electric field and wave experiment," in *The Cluster Mission-Scientific and Technical Aspects of the Instruments*, **ESA SP-1103**, p. 31, ESA Publications Div., Noordwijk, The Netherlands, 1988.

Mangeney, A., et al., WIND observations of coherent electrostatic waves in the solar wind, *Annales Geophysicae*, **17**, 307, 1999.

Matsumoto, H. et al., Electrostatic solitary waves (ESW) in the magnetotail: BEN waveforms observed by Geotail, *Geophys. Res. Lett*., **21**, 2915, 1994.

Matsumoto, H. et al., Generation mechanism of ESW based on the GEOTAIL Plasma Wave Observation, Plasma Observation and Particle Simulation, *Geophys. Res. Lett*., **26**, 421-424, 1999.

Mottez, F. et al., Coherent structures in the magnetotail triggered by counterstreaming electron beams, *J. Geophys. Res*., 102, 11399, 1997.

Mozer, F. et al., New features in time domain electric field structures in the auroral acceleration region, *Phys. Rev. Lett.*, **79**, 1281, 1997.

Muschietti, L. et al., Phase-space electron holes along magnetic field lines, *Geophys. Res. Lett*., **26**, 1093, 1999.

Omura, Y. et al., Electron beam instabilities as the generation mechanism of electrostatic solitary waves in the magnetotail, *J. Geophys. Res*, **101**, 2685-2697, 1996.

Pedersen, A., Solar wind and magnetospheric plasma diagnostics by spacecraft electrostatic potential measurements, *Annales Geophysicae*, **13**, 118 1995.

Russell, C. T. et al., The GGS/Polar Magnetic Fields Investigation, in *The Global Geospace Mission*, C.T. Russell, ed., p. 563, 1995.

Scudder, J. et al., Hydra- A 3-d electron and ion hot plasma instrument for the Polar spacecraft of the GGS mission, in *The Global Geospace Mission*, C.T. Russell, ed., p. 459, 1995.

Shelley, E. G. *et al*., The Toroidal Imaging Mass-Angle Spectrograph (TIMAS) for the Polar Mission, in *The Global Geospace Mission*, C.T. Russell, ed., p. 497, 1995.

Temerin, M. et al., Observations of solitary waves and double layers in the auroral plasma, *Phys. Rev. Lett.*, **48**, 1175, 1982.

Treumann, R., J. LaBelle and T. Bauer, Diffusion Processes: An Observational Perspective, in *Physics of the Magnetopause*, Geophys. Mon. **90**, AGU P. Song, B. Sonnerup and M. Thomsen, eds., pg. 331, 1995.

Tsurutani, B., J. Arballo, G. Lakhina, C. Ho, B. Buti, J. Pickett, and D. Gurnett, Plasma waves in the dayside polar cap boundary layer: Bipolar and monopolar eletric pulses and whistler mode waves, *Geophys. Res. Lett*., **25**, 4117, 1998.

Figure Captions

Figure 1. A magnetopause crossing on 4/2/2001. From top to bottom the panels are : The negative of the spacecraft potential; and the magnitude of the magnetic field and the three components of the magnetic field in GSM; the three magnetic field-aligned components of the electric field during the waveform capture; and an expanded view of the field-aligned component of the electric field for 0.12s to show an example of the solitary waves.

Figure 2. The x and z components of the electric field and the x component of the search coil magnetic field data in field-aligned coordinates and their Fourier transforms from the waveform capture on 4/2/2001.

Figure 3. A magnetopause crossing on 3/23/2001. From top to bottom the panels are: The negative of the spacecraft potential; the magnitude of the magnetic field and the three components of the magnetic field in GSM; and an expanded view of the field-aligned component of the electric field for 0.12s to show an example of the solitary waves.

Figure 4. Another magnetopause crossing on 3/23/2001. Same format as Fig. 3.

Figure 5. A histogram of the solitary wave speed for the three spatial regions. Note that 'Inf' refers to cases which were moving so rapidly (usually >2500 km/s) that no time delay could be measured.

Figure 6. A histogram of the amplitude of the solitary waves for all the high altitude events . Events plotted in black correspond to the 'Inf' cases and represent a minimum potential.

Figure 7. A scatter plot of amplitude versus width for all the high altitude solitary wave events.

Figure 8. Solitary waves and associated wave packets on 3 satellites on March 7, 2001 at ~8.2 Re and ~9 MLT in the region of the cusp. (a) Overview of the complete waveform capture with 1 component of the electric field from SC2, SC3, and SC4 and the Fourier spectra; (b), (c) and (d) Shorter snapshots within the burst, showing solitary waves.

Figure 9. Waveform capture obtained on March 3, 2001 at ~(12, 3, 9) Re near noon, close to the bow shock: (a). Plot of the 2 electric field components and the spacecraft potential (indicative of density) observed on the 4 satellites; (b) and (c) Shorter snapshots.

Figure 10. One component of the waveform capture electric field data from the four satellites on March 31, 2001 near the plasma sheet boundary.

Figure 11. An approximately 0.03 second interval from each satellite (note each interval is at a different time).

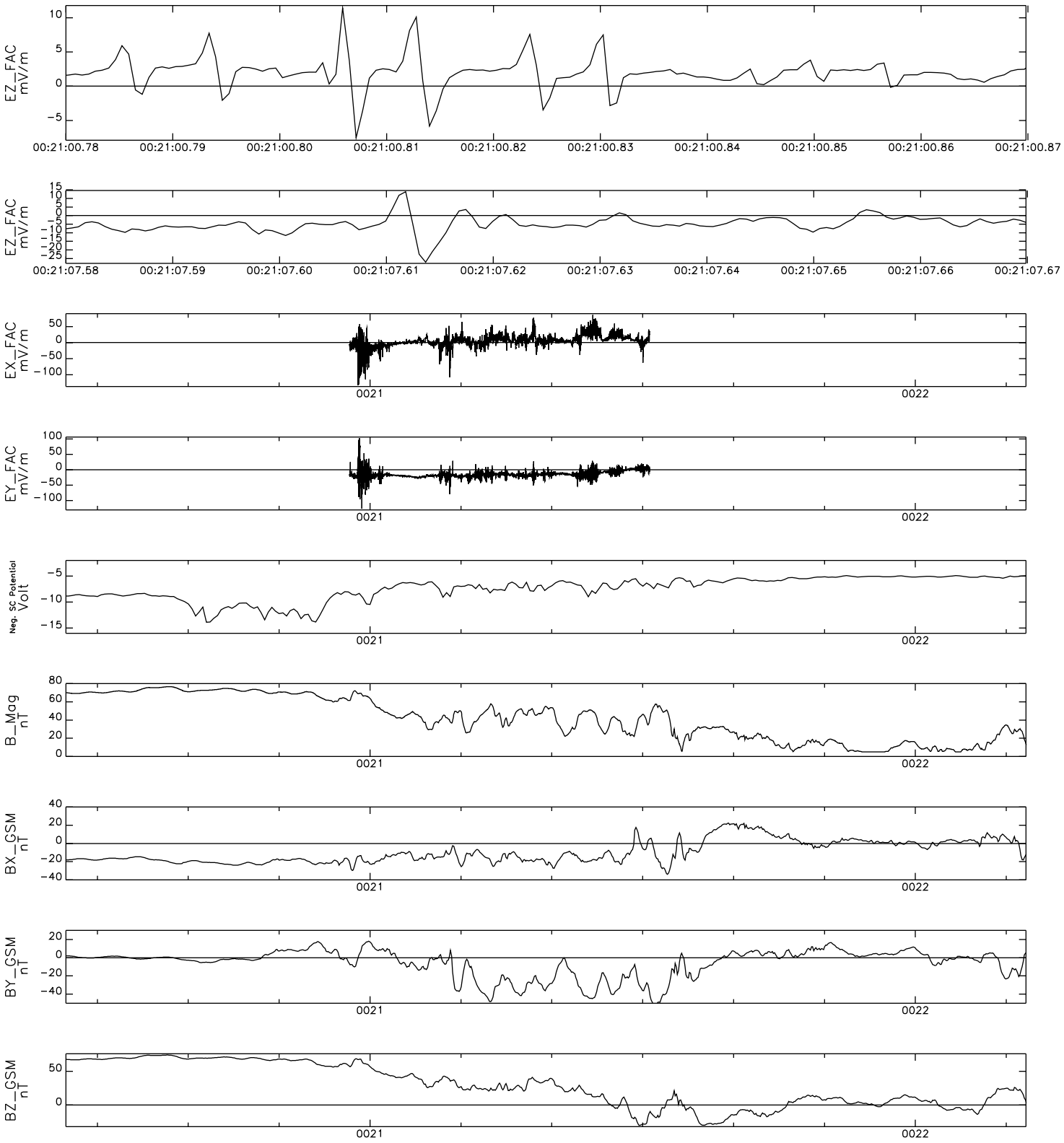

Time:	00:21:18.0	00:21:18.1	00:21:18.2	00:21:18.3	00:21:18.4	00:21:18.5	00:21:18.6	00:21:18.7	00:21:18.8
Re	9.41	9.41	9.41	9.41	9.41	9.41	9.41	9.41	9.41
MLT	11.59	11.59	11.59	11.59	11.59	11.59	11.59	11.59	11.59
MLat	12.09	12.09	12.09	12.09	12.09	12.09	12.09	12.09	12.09
LShell	9.77	9.77	9.77	9.77	9.77	9.77	9.77	9.77	9.77

P:<SDT>, V:<2.4> T:<Fri Sep 7 10:09:23 2001>; Cfg=magnetopause_fig1_2apr

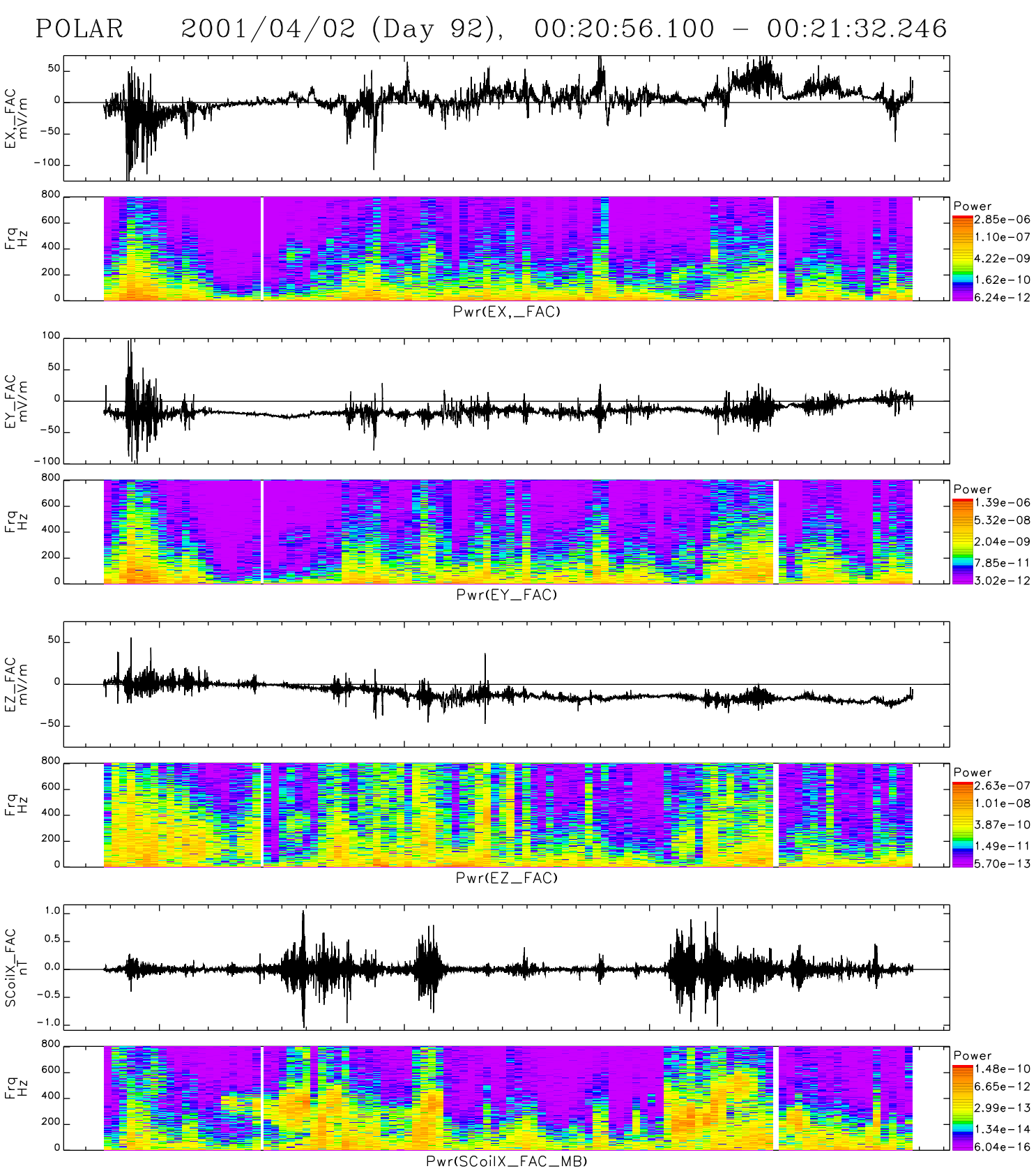

Time:	00:21:00	00:21:10	00:21:20	00:21:30
Re	9.41	9.41	9.41	9.41
MLT	11.59	11.59	11.59	11.59
MLat	12.08	12.08	12.09	12.10
LShell	9.77	9.77	9.77	9.77

P:<SDT>, V:<2.4> T:<Thu Aug 23 16:44:04 2001>; Cfg=magnetopause_fig1a

POLAR 2001/03/23 (Day 82), 01:36:18.021 – 01:36:18.052

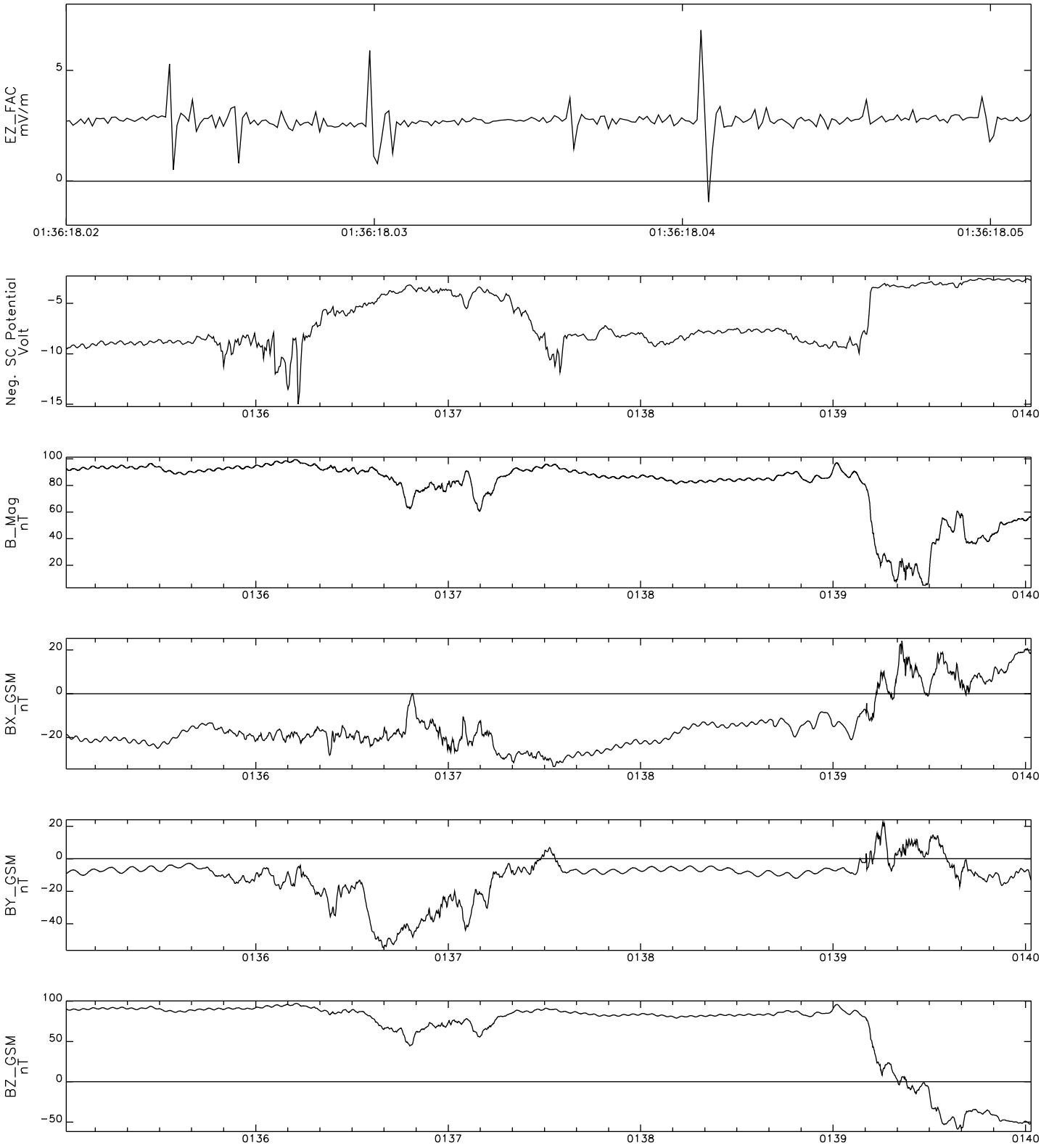

Time:	0136	0137	0138	0139	0140
Re	9.09	9.10	9.10	9.11	9.11
MLT	12.17	12.17	12.17	12.17	12.17
MLat	6.07	6.12	6.17	6.21	6.26
LShell	9.12	9.13	9.14	9.14	9.15

P:<SDT>, V:<2.4> T:<Thu Sep 6 12:02:39 2001>; Cfg=tromso_fig3_23mar

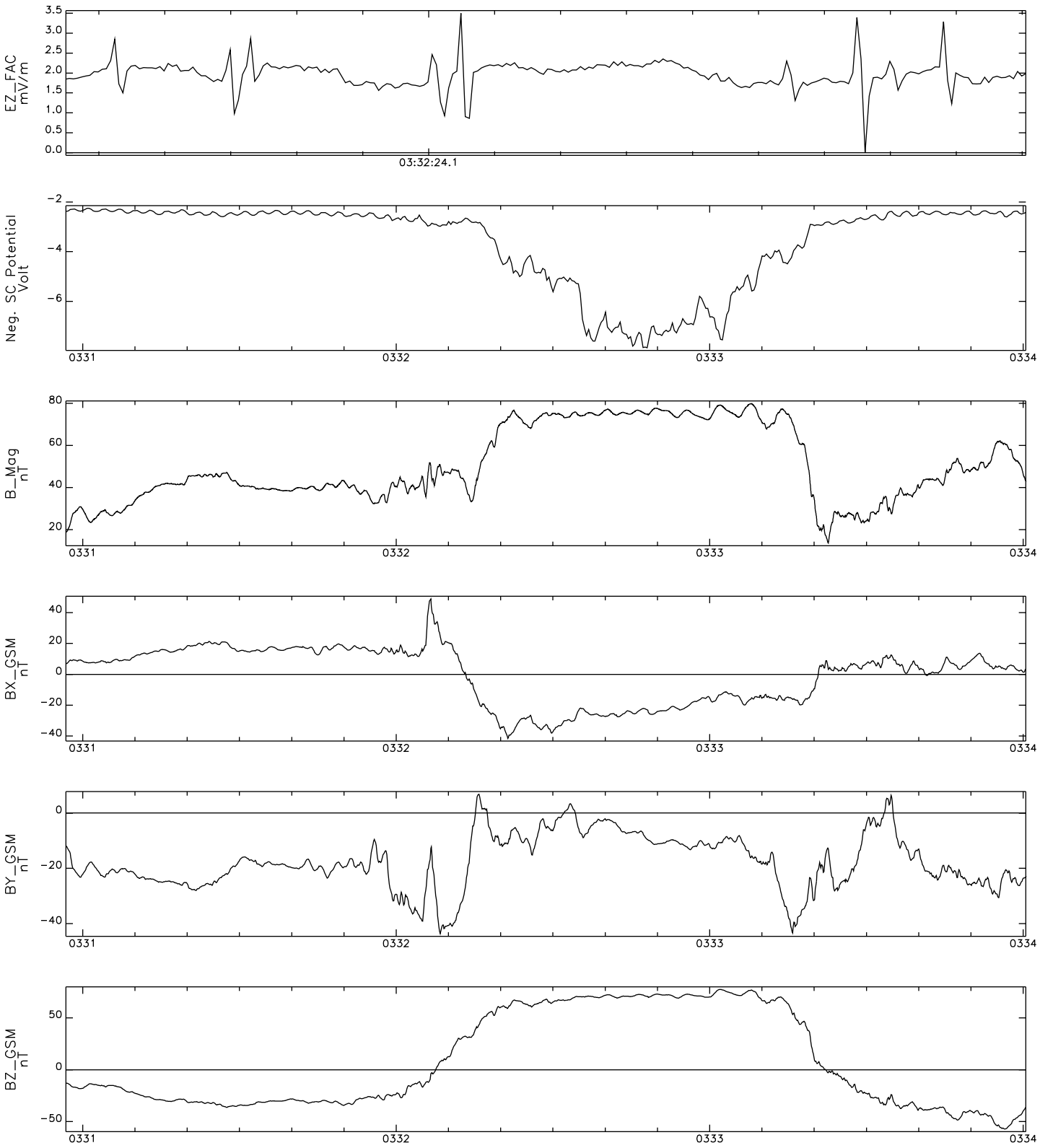

Time:	03:32:24.1
Re	9.47
MLT	12.23
MLat	12.13
LShell	9.83

P:<SDT>, V:<2.4> T:<Thu Sep 6 12:02:39 2001>; Cfg=tromso_fig3_23mar

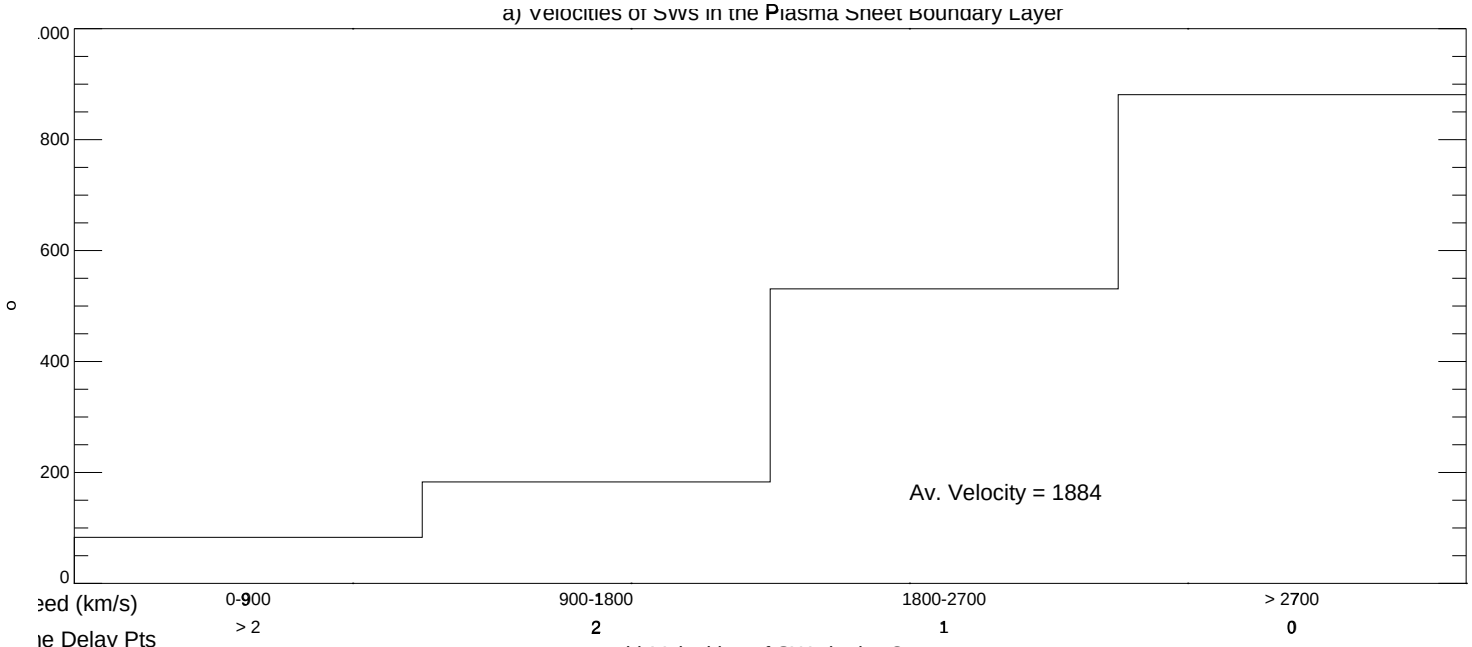
a) Velocities of SWs in the Plasma Sheet Boundary Layer
000
800
600
400
200
0
o
Av. Velocity = 1884
0-900
900-1800
1800-2700
> 2700
> 2
2
1
0

ed (km/s)
e Delay Pts

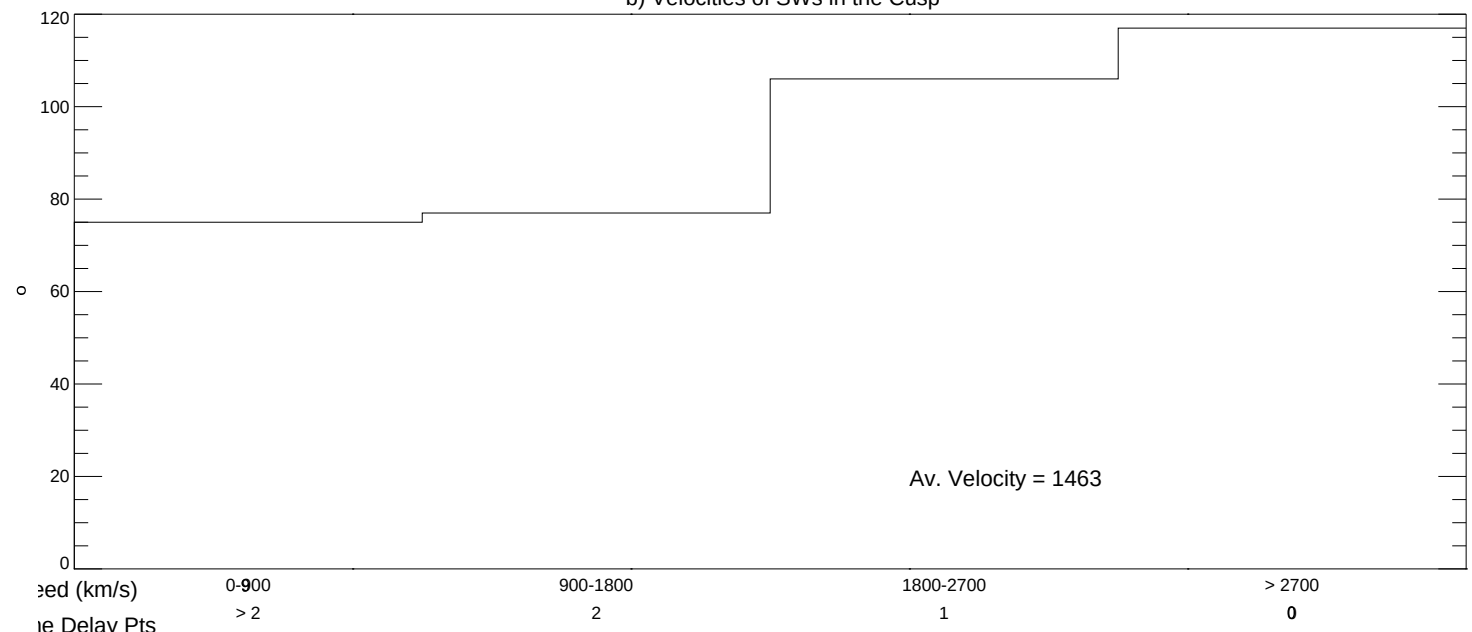
b) Velocities of SWs in the Cusp
120
100
80
60
40
20
0
o
Av. Velocity = 1463
0-900
900-1800
1800-2700
> 2700
> 2
2
1
0

ed (km/s)
e Delay Pts

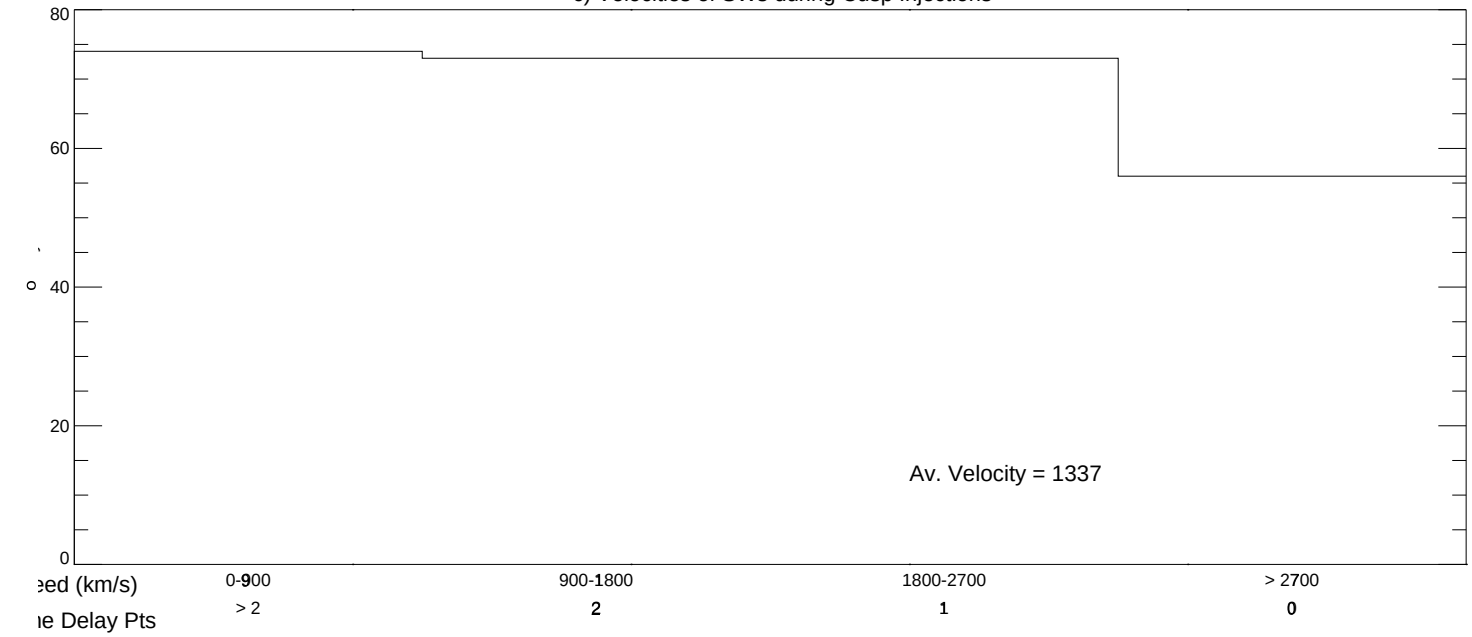
c) Velocities of SWs during Cusp Injections
80
60
40
20
0
o
Av. Velocity = 1337
0-900
900-1800
1800-2700
> 2700
> 2
2
1
0

ed (km/s)
e Delay Pts

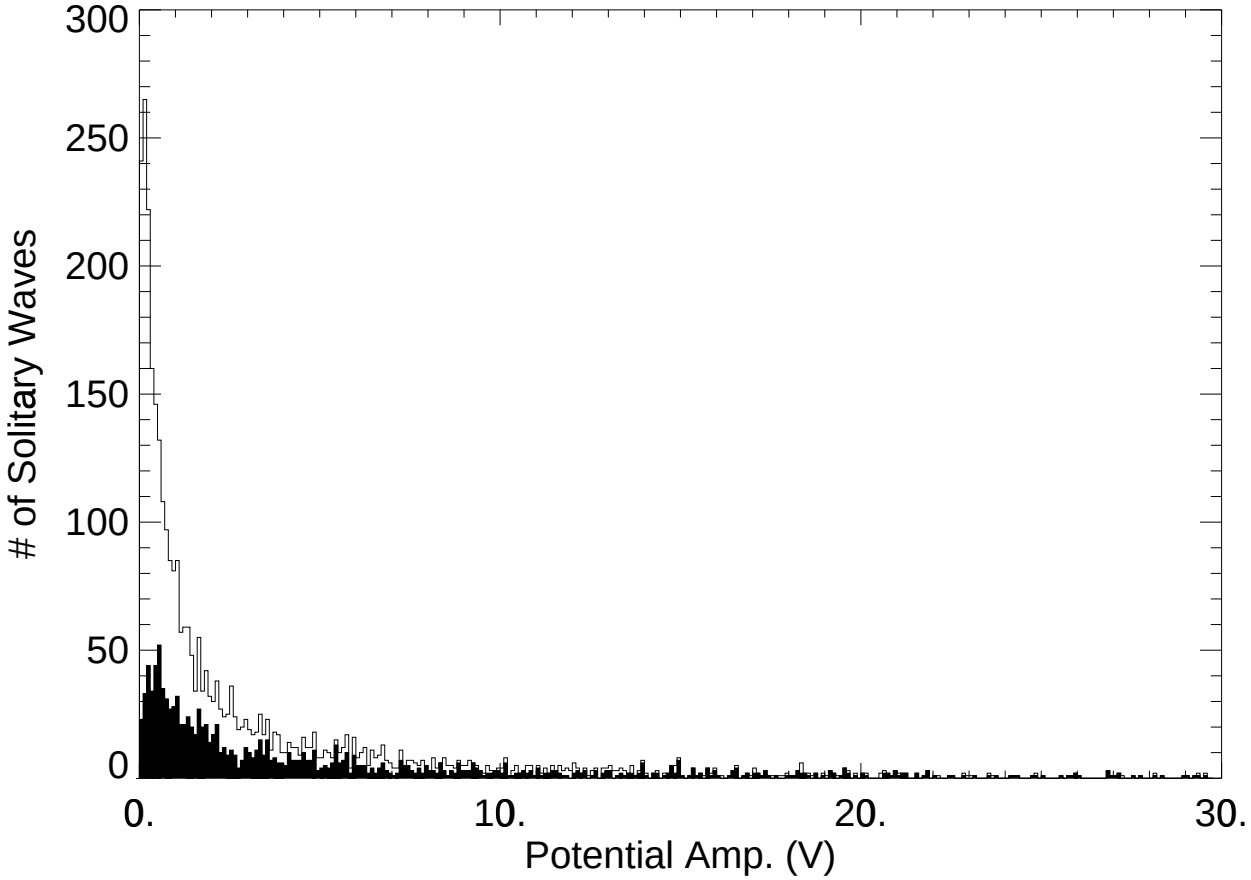

<Vers. 1.91 - Fri Sep 14 16:04:12 2001>

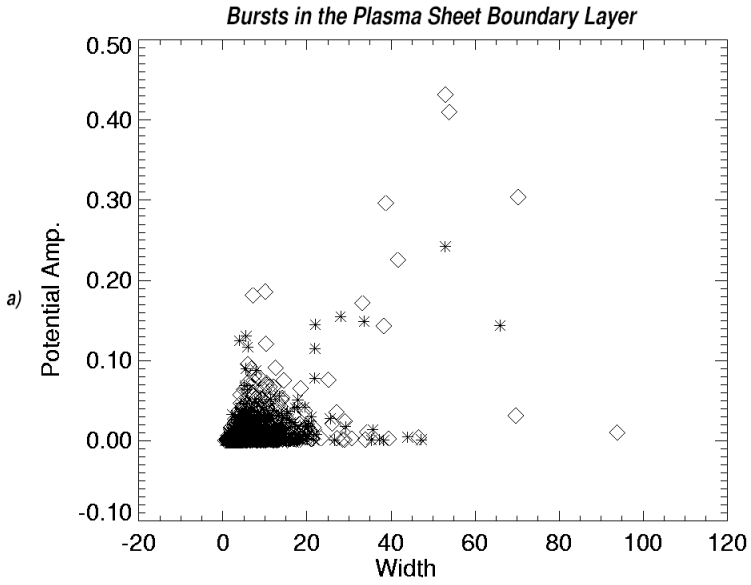
Bursts in the Plasma Sheet Boundary Layer
a)
Potential Amp.
0.50
0.40
0.30
0.20
0.10
0.00
-0.10
-20
0
20
40
60
80
100
120
Width

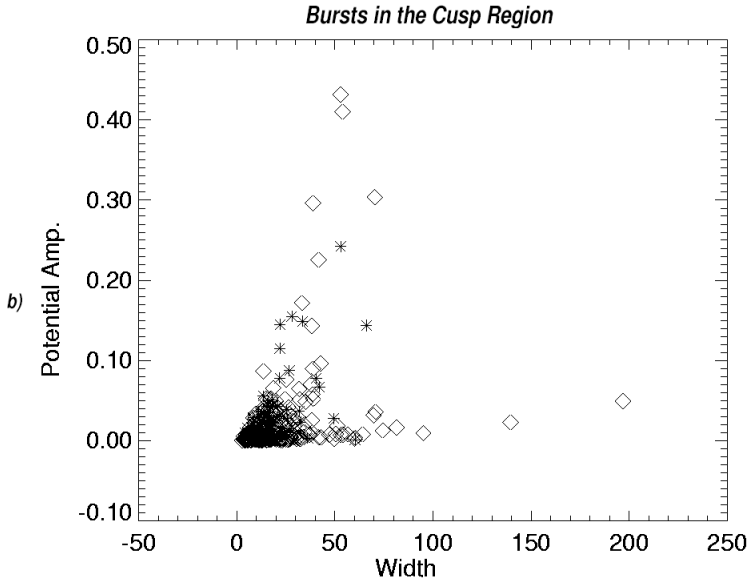
Bursts in the Cusp Region
b)
Potential Amp.
0.50
0.40
0.30
0.20
0.10
0.00
-0.10
-50
0
50
100
150
200
250
Width

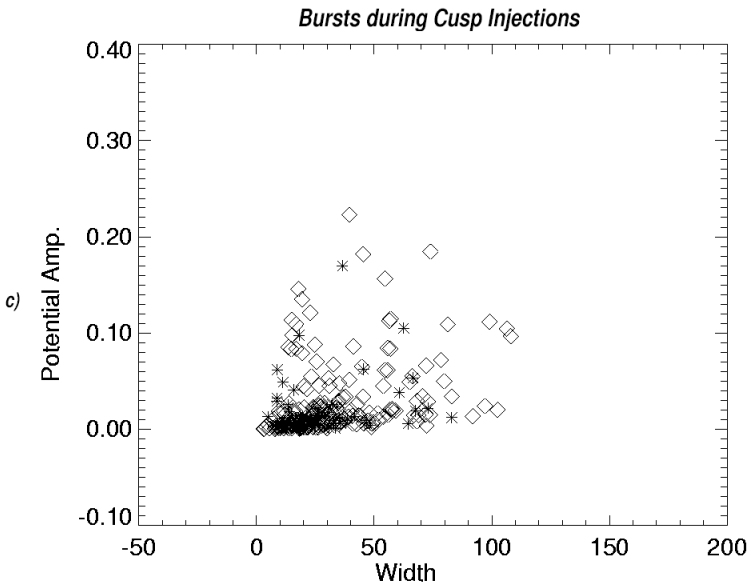
Bursts during Cusp Injections
c)
Potential Amp.
0.40
0.30
0.20
0.10
0.00
-0.10
-50
0
50
100
150
200
Width

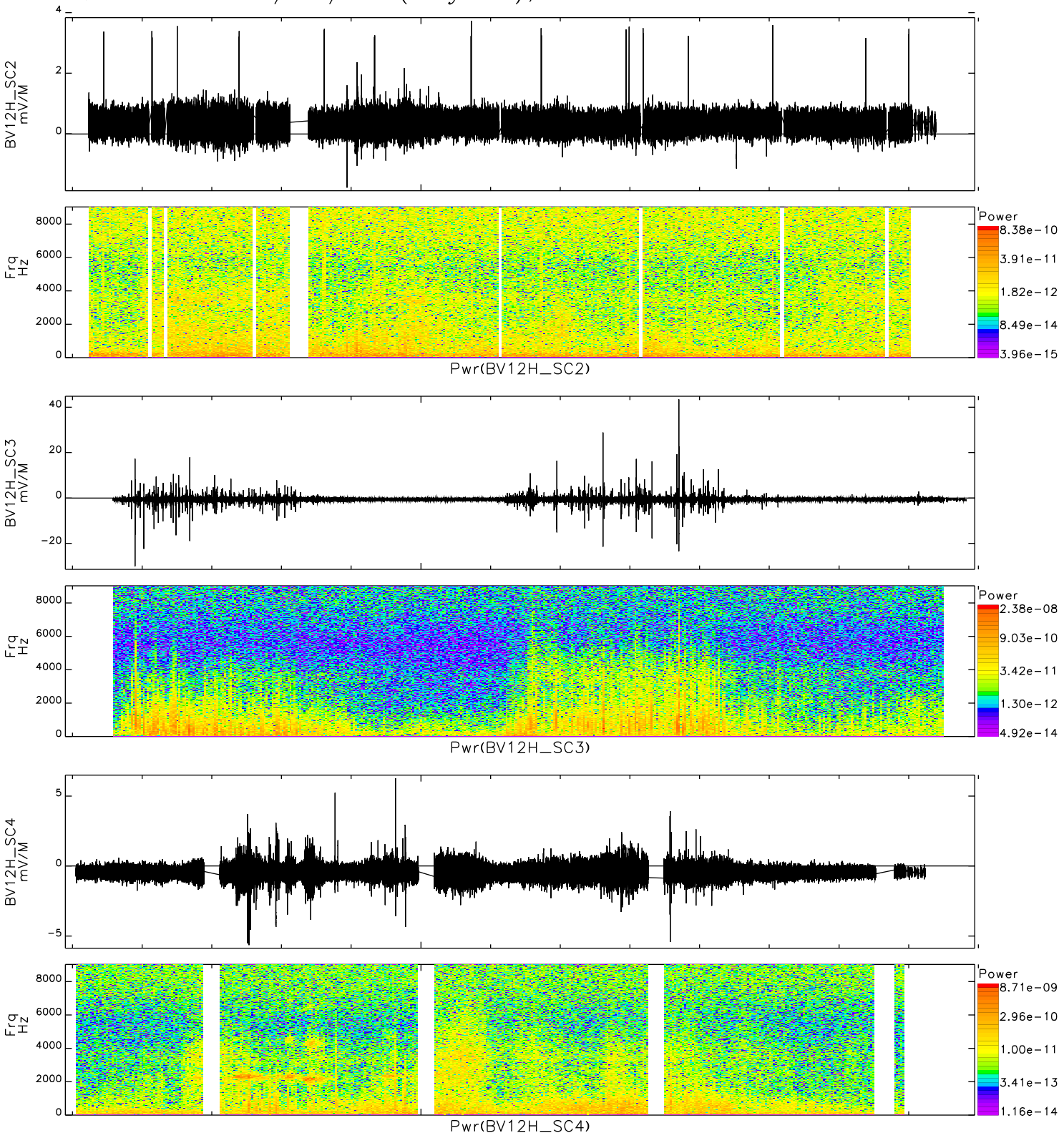

Time:	07:28:00
Re	8.20
Lat	−74.47
MLT	8.88
ILat	86.16
LShell	223.10

P:<SDT>, V:<3.5> T:<Thu Sep 13 10:13:28 2001>; Cfg=Vsc_BVH

Cluster 2001/03/07 (Day 66), 07:27:57.902 – 07:27:57.970

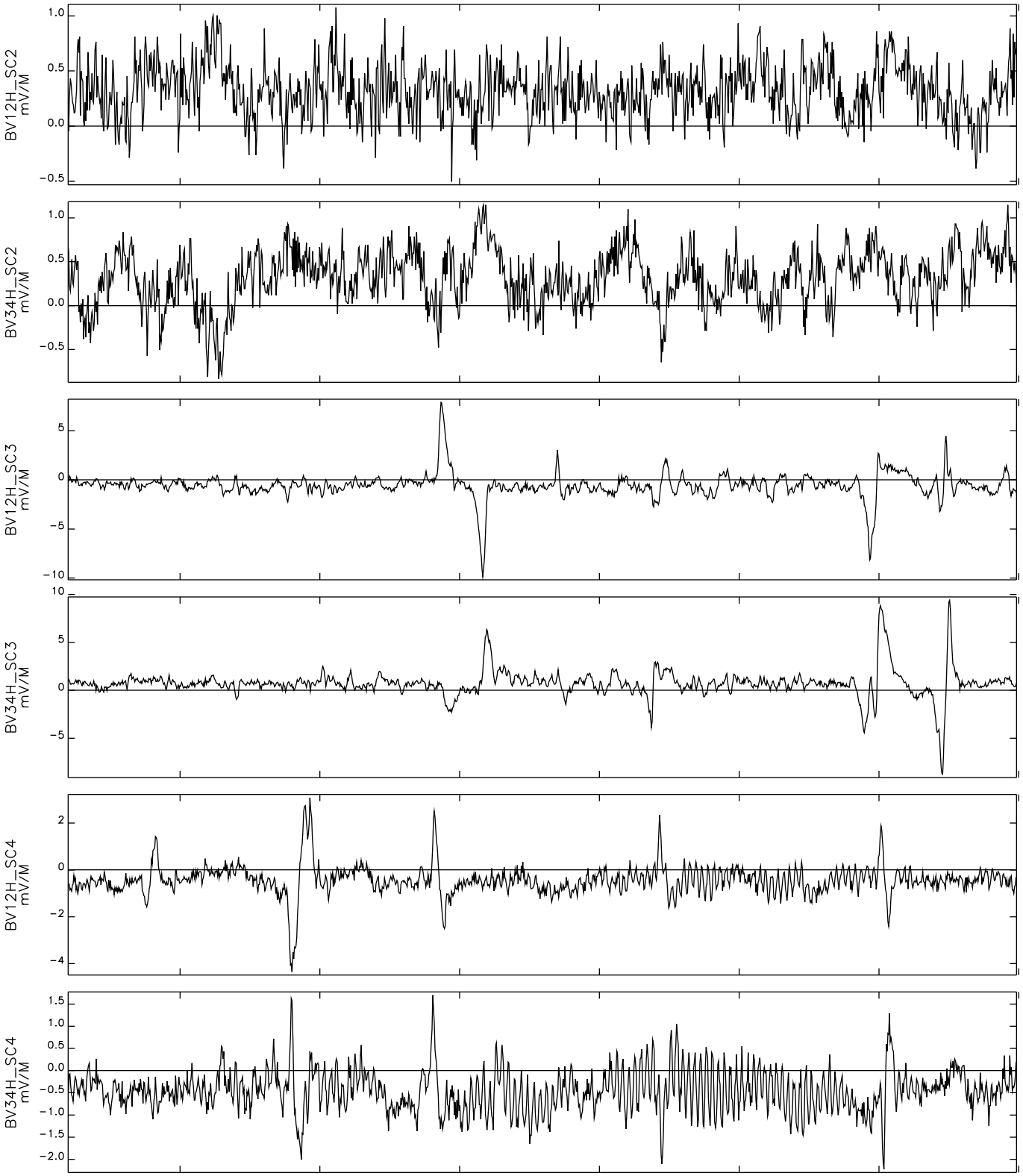

Time:	07:27:57.91	07:27:57.92	07:27:57.93	07:27:57.94	07:27:57.95	07:27:57.96
Re	8.20	8.20	8.20	8.20	8.20	8.20
Lat	−74.46	−74.46	−74.46	−74.46	−74.46	−74.46
MLT	8.88	8.88	8.88	8.88	8.88	8.88
ILat	86.16	86.16	86.16	86.16	86.16	86.16
LShell	223.02	223.02	223.02	223.02	223.02	223.02

P:<SDT>, V:<3.5> T:<Thu Sep 13 10:13:28 2001>; Cfg=Vsc_BVH

Cluster 2001/03/07 (Day 66), 07:28:03.303 – 07:28:03.358

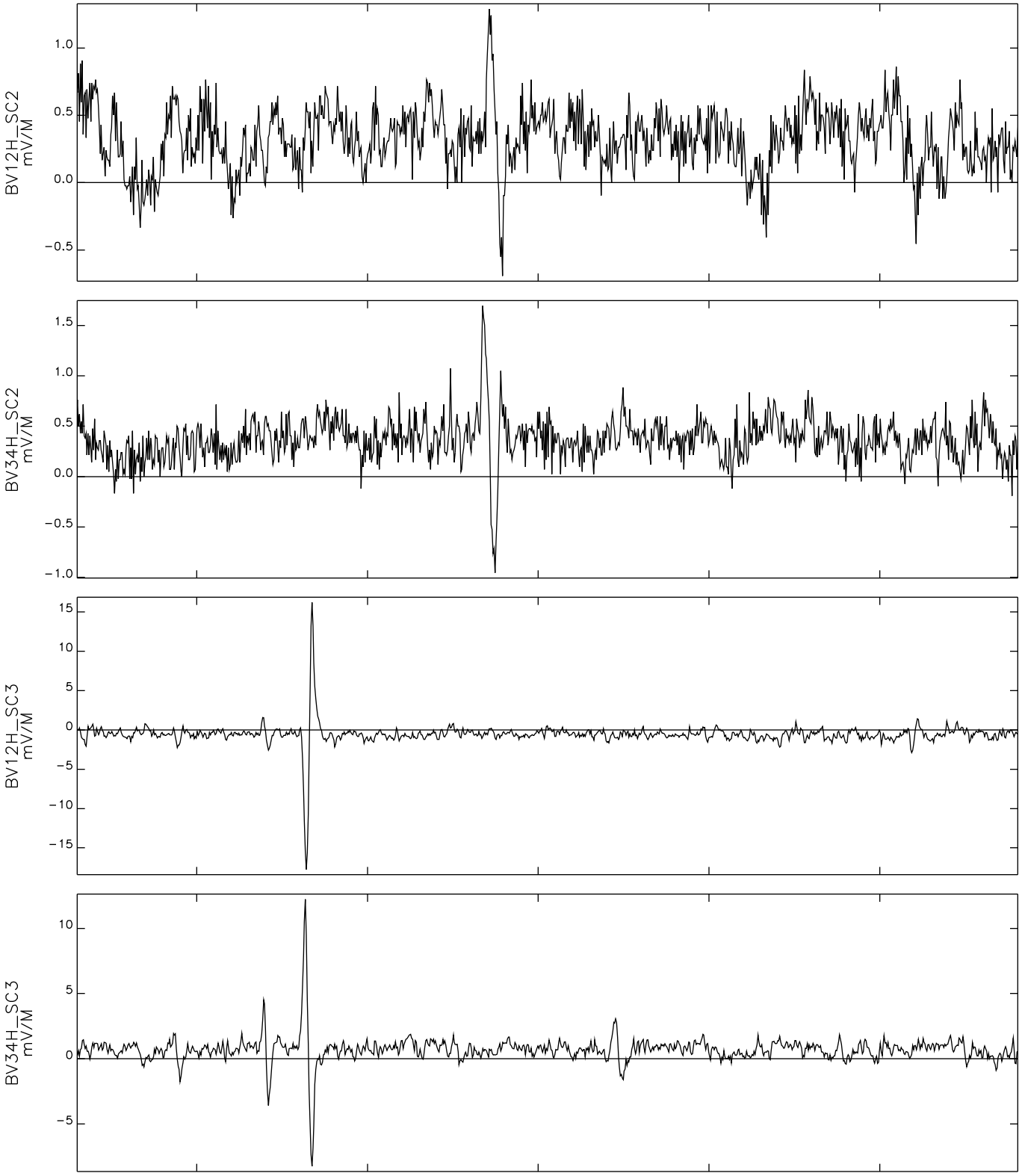

Time:	07:28:03.31	07:28:03.32	07:28:03.33	07:28:03.34	07:28:03.35
Re	8.20	8.20	8.20	8.20	8.20
Lat	−74.48	−74.48	−74.48	−74.48	−74.48
MLT	8.88	8.88	8.88	8.88	8.88
ILat	86.16	86.16	86.16	86.16	86.16
LShell	223.23	223.23	223.23	223.23	223.23

P:<SDT>, V:<3.5> T:<Thu Sep 13 10:13:28 2001>; Cfg=Vsc_BVH

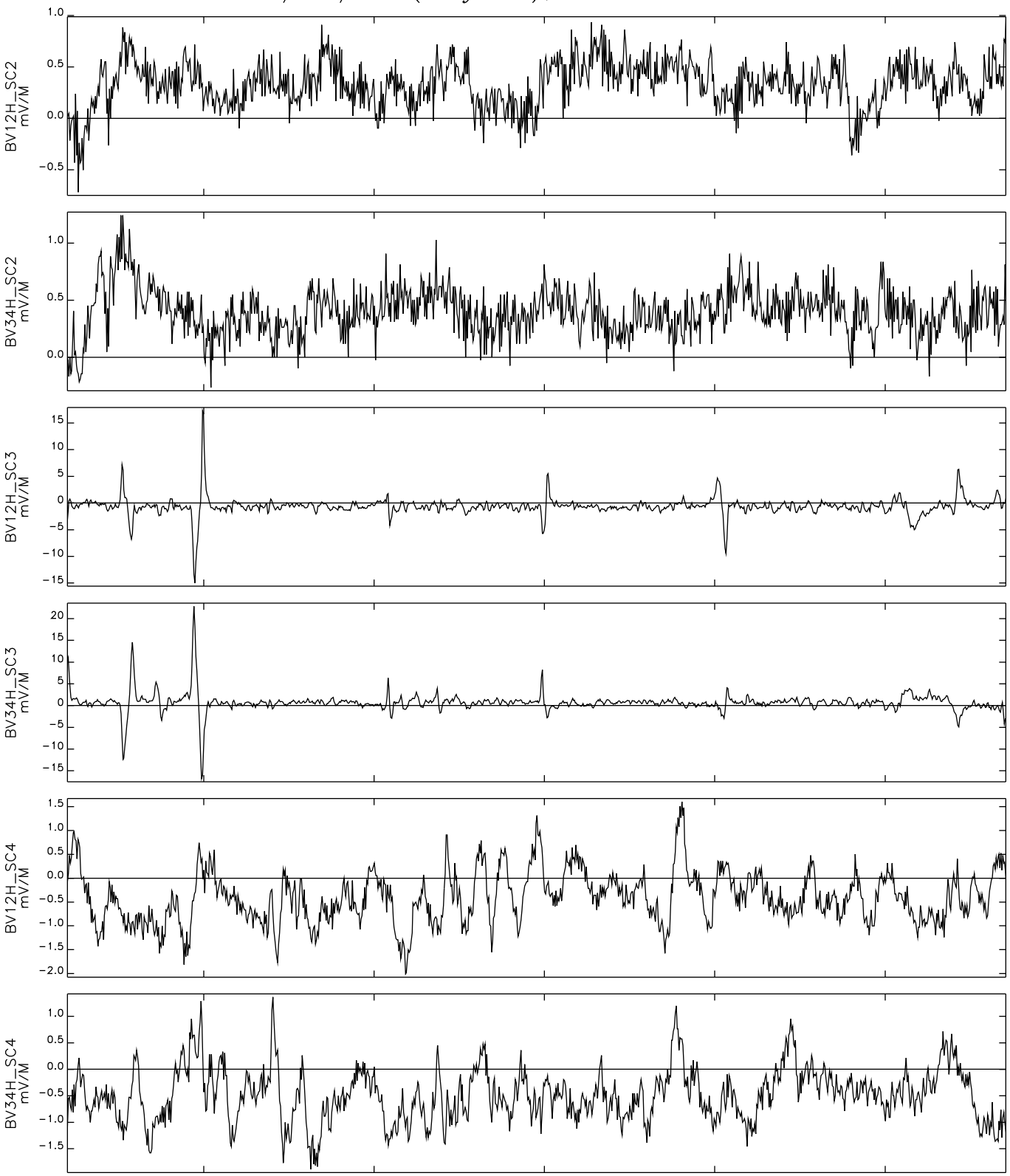
Cluster 2001/03/07 (Day 66), 07:28:03.083 – 07:28:03.138
BV12H_SC2 mV/M
BV34H_SC2 mV/M
BV12H_SC3 mV/M
BV34H_SC3 mV/M
BV12H_SC4 mV/M
BV34H_SC4 mV/M
Time: 07:28:03.09 07:28:03.10 07:28:03.11 07:28:03.12 07:28:03.13
Re 8.20 8.20 8.20 8.20 8.20
Lat −74.48 −74.48 −74.48 −74.48 −74.48
MLT 8.88 8.88 8.88 8.88 8.88
ILat 86.16 86.16 86.16 86.16 86.16
LShell 223.22 223.22 223.22 223.22 223.22
P:<SDT>, V:<3.5> T:<Thu Sep 13 10:13:28 2001>; Cfg=Vsc_BVH

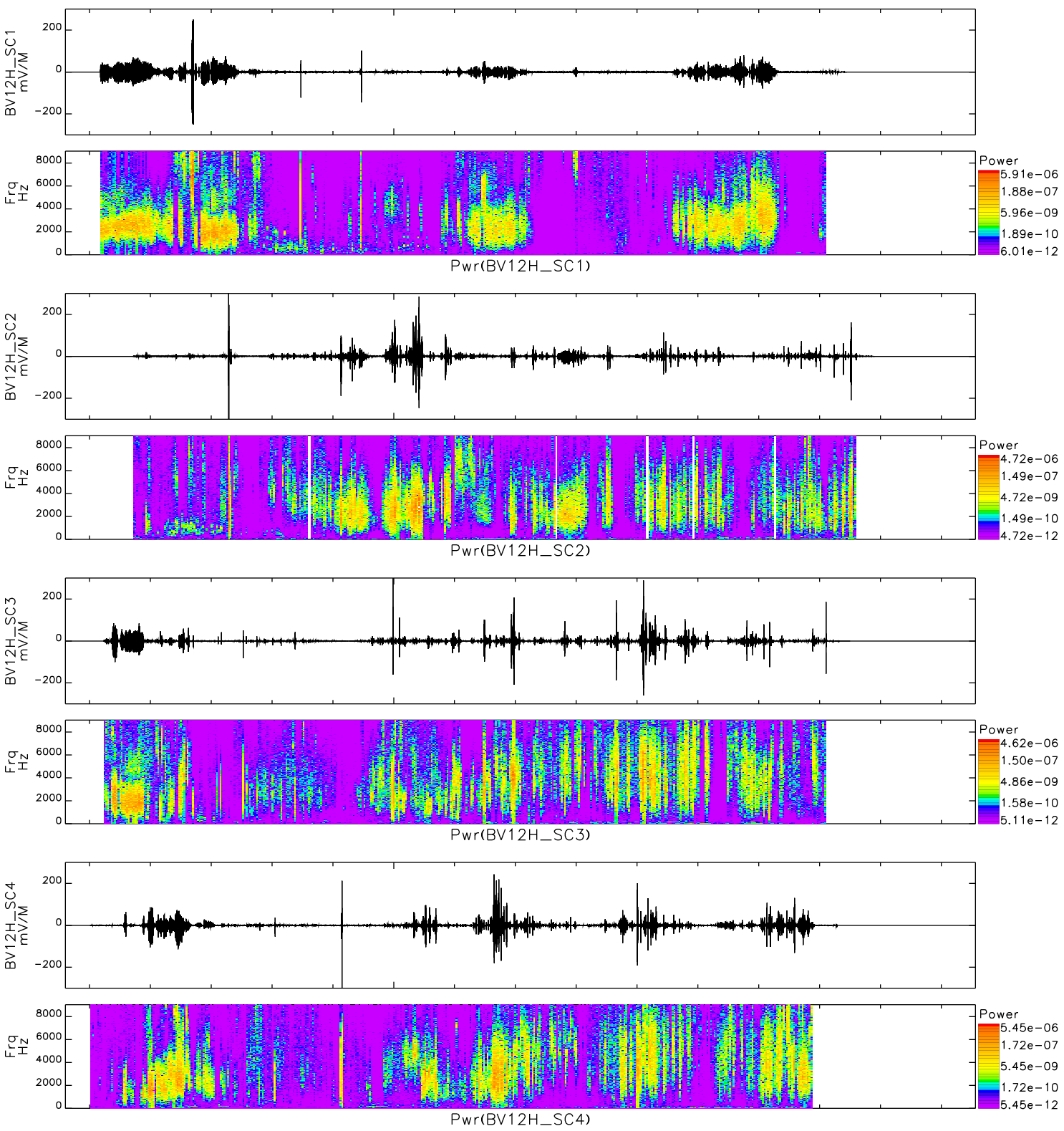

Time:	07:17:00
Re	15.51
Lat	29.56
MLT	12.10
ILat	—
LShell	—

P:<SDT>, V:<3.5> T:<Wed Sep 12 11:58:38 2001>; Cfg=march3_all4vscbv

Cluster 2001/03/03 (Day 62), 07:17:05.401 – 07:17:06.999

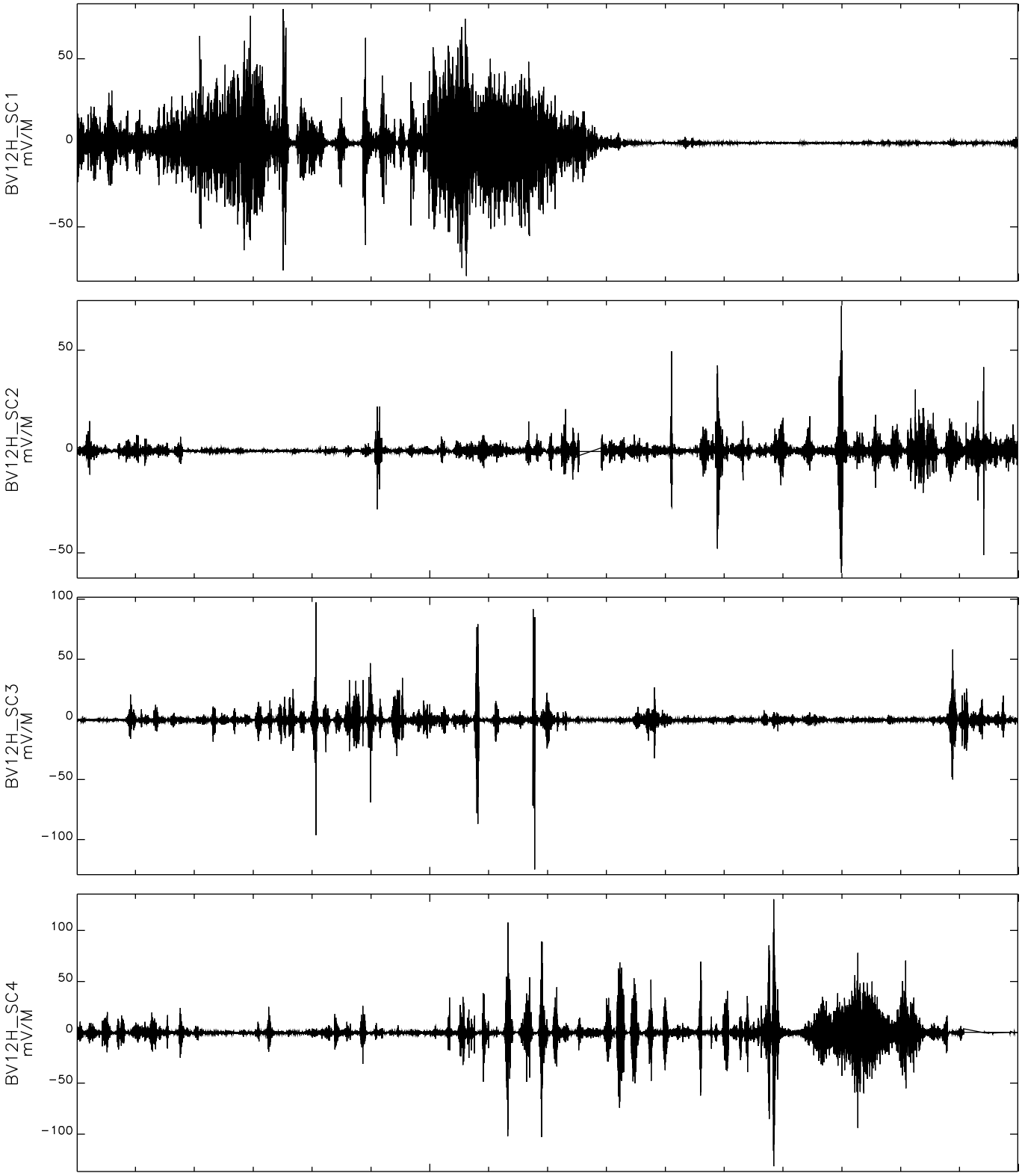

Time:	07:17:06
Re	15.51
Lat	29.56
MLT	12.10
ILat	—
LShell	—

P:<SDT>, V:<3.5> T:<Wed Sep 12 11:58:38 2001>; Cfg=march3_all4vscbv

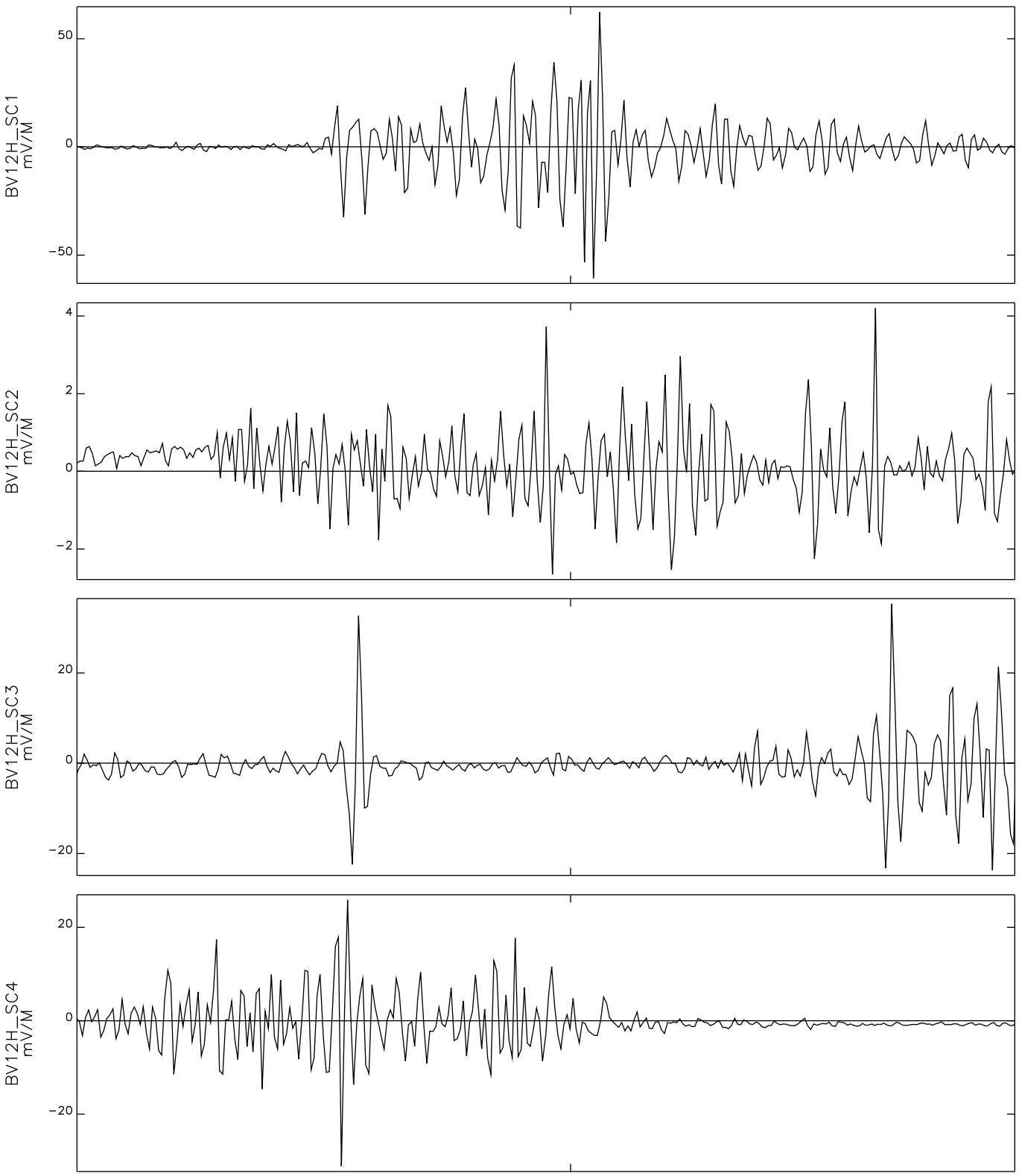

Time:	07:17:05.89
Re	15.51
Lat	29.56
MLT	12.10
ILat	—
LShell	—

P:<SDT>, V:<3.5> T:<Wed Sep 12 11:58:38 2001>; Cfg=march3_all4vscbv

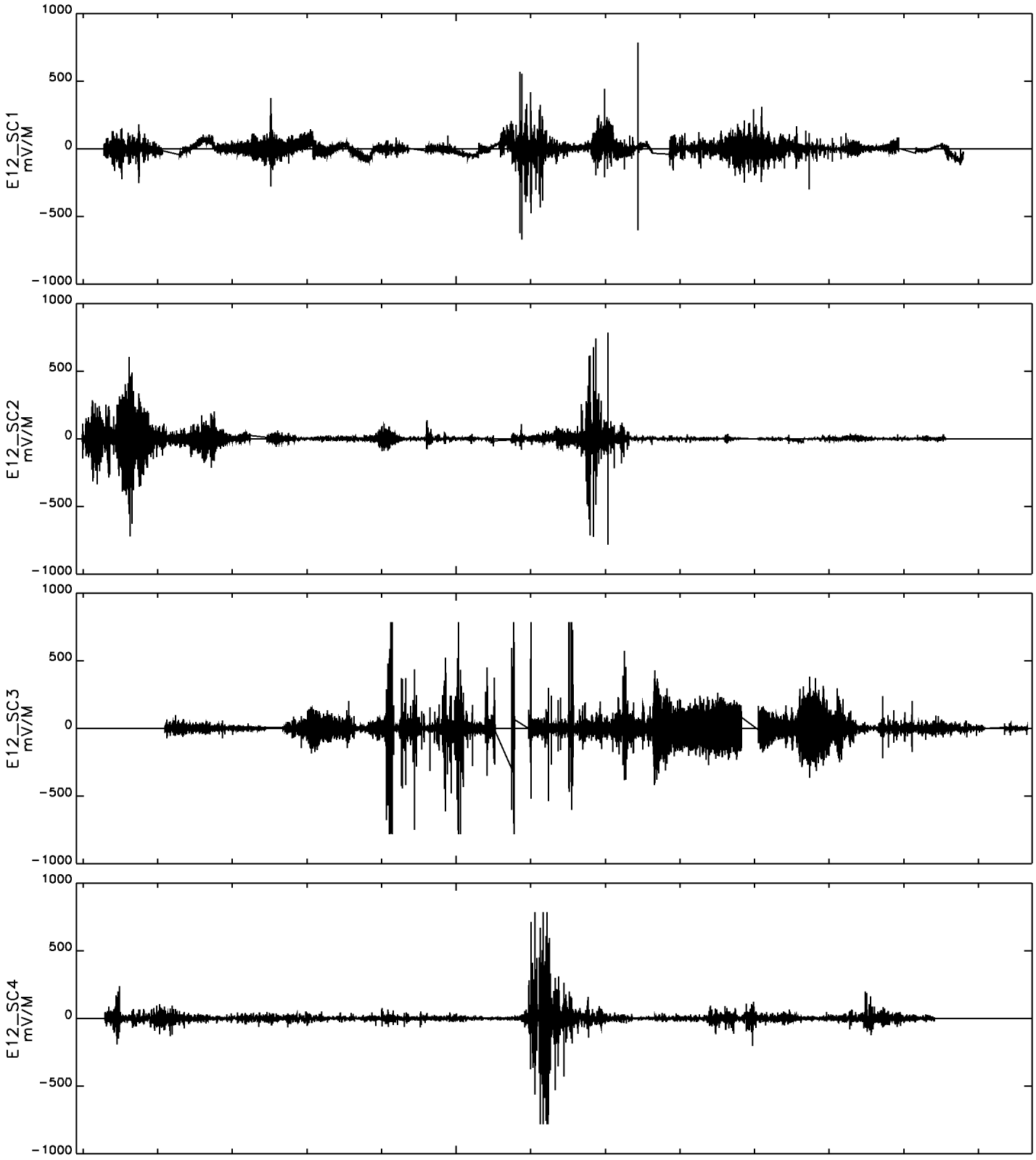
Cluster 2001/03/31 (Day 90), 06:43:54.911 - 06:44:07.720
E12_SC1 mV/M
E12_SC2 mV/M
E12_SC3 mV/M
E12_SC4 mV/M
1000
500
0
-500
-1000
Time: 06:44:00
Re 4.16
Lat -19.78
MLT
ILat
LShell
P:<SDT>, V:<3.5> T:<Wed Nov 21 16:18:39 2001>

Cluster 2001/03/31 (Day 90), 06:44:00.849 – 06:44:00.881

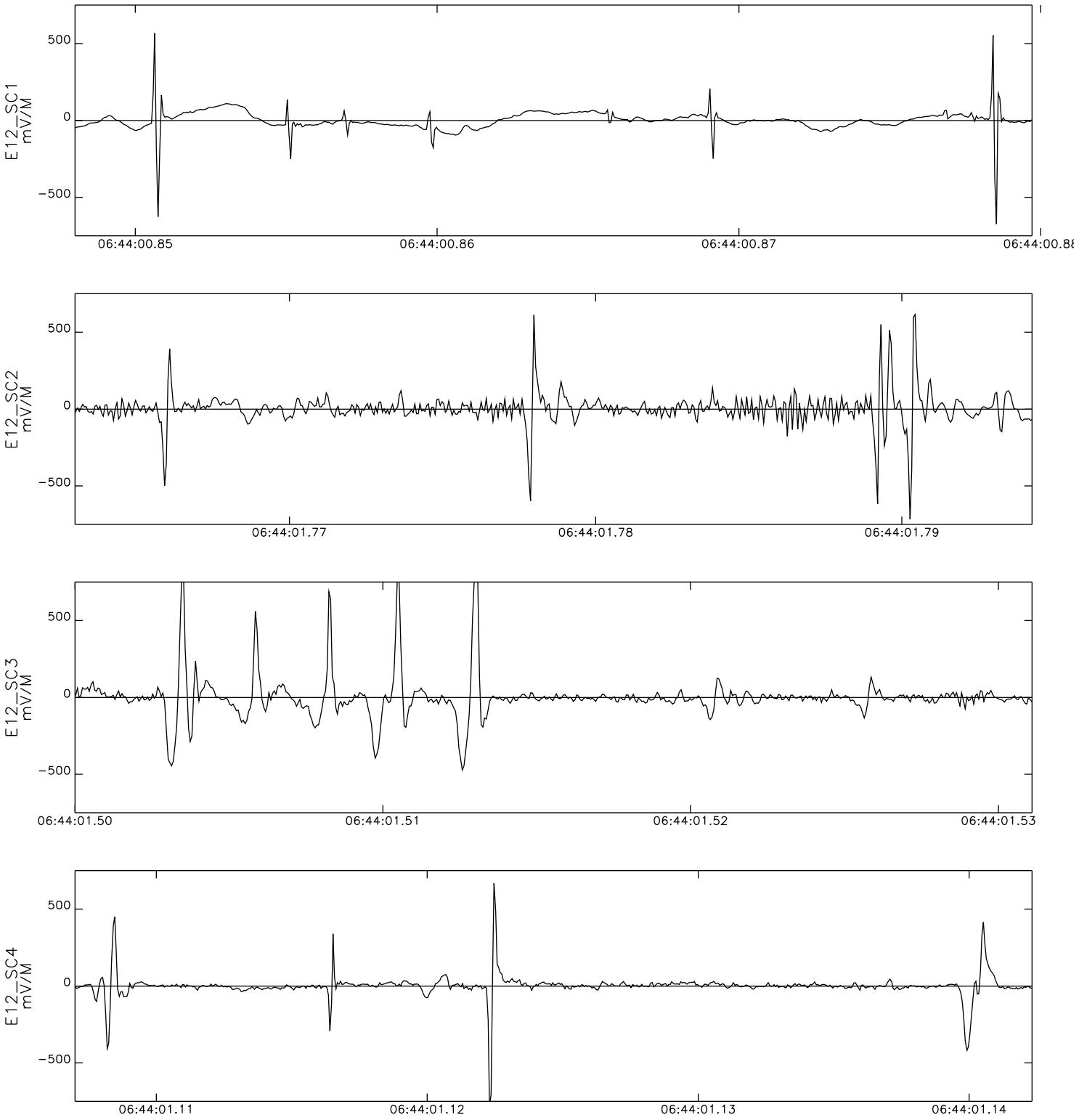

Time:	06:44:01	06:44:02
Re	4.16	4.16
Lat	−19.77	−19.76
MLT		
ILat		
LShell		

P:<SDT>, V:<3.5> T:<Wed Nov 21 16:18:39 2001>